Fast Synchronization Algorithm of High-Stability Oscillators to GNSS Signals

Paweł Kubczak, Mieczysław Jessa, Michał Kasznia

Institute of Multimedia Telecommunications
Poznan University of Technology
Poznan, Poland
pawel.kubczak@put.poznan.pl, mieczyslaw.jessa@put.poznan.pl, michal.kasznia@put.poznan.pl

Summary—**The paper describes the algorithm for fast synchronization of atomic oscillators. The algorithm performance controlling the LPFRS oscillator is compared to the algorithm built in the CSAC. The experiments' results confirm the proposed method's capabilities to obtain synchronization times lower than for algorithms built into the CSAC oscillator while ensuring comparable or better quality.**

Keywords— synchronization; GNSS; rubidium oscillator, CSAC

I. INTRODUCTION

Fast frequency and phase synchronization of oscillators with daily frequency instability of not more than 10^{-9} to 1PPS signals coming from Global Satellite Navigation Systems (GNSS) are one of the basic problems to be solved in military applications, IoT devices, or 5G networks. The output signal must achieve the assumed quality as soon as possible and keep it in long time intervals. The transition of the control algorithm into the HOLDOVER state, i.e., the state of synchronization maintenance after the loss of the 1PPS signal, must be precise, and the return from the HOLDOVER to synchronism after the input signal is present should be as soon as possible and without significant loss of quality during the transition state. A control algorithm built into a chip scale cesium clock CSAC [1] was chosen as a reference solution to evaluate the proposed algorithm's quality.

Fast synchronization is most often used during synchronization and location measurements in the field. Instead of carrying a heavy and expensive battery-backed atomic standard and waiting for it to reach thermal stability, which lasts at least 15 minutes, we get the frequency and phase of the local generator synchronized with the GNSS signal at the same time. In the synchronized state, the local generator provides a reference signal with parameters comparable to portable cesium standards. The reference source synchronized to GNSS is significantly cheaper, smaller, lighter, and more mobile. The disadvantage of the device is that the quality of operation substantially depends on the external factor – the availability and quality of the GNSS signal.

The speed of access to synchronization is also critical in military applications. The success of military operations, and thus also the lives of soldiers, often depends on achieving quick synchronization. The smaller the phase error is, we are able to achieve the greater the spatial accuracy of the navigation. It is not only about navigation in the field and recognizing the location of allied units but also about precise navigation of missiles with an accuracy of several centimeters. Ensuring fast and stable synchronization is also necessary to transfer large amounts of telemetry data and provide communication.

Fast synchronization is also essential in the event of a telecommunications network failure. The sooner you can recover sync, the sooner you can restore your data transmissions. Maintaining the continuity of the network is very important for the operator because it is closely related to profits.

Fast synchronization is also needed for the Internet of Things (IoT), especially for mobile devices, which currently widely use GNSS signals. You can imagine a situation in which a mobile device is brought into a building and loses its GNSS signal. Then, when the building is lowered, and the GNSS signal is available again, there is a need to ensure fast synchronization again, as the small and low-cost device does not have a stable frequency source that could provide backup during the unavailability of the GNSS signal. The use of fast synchronization, in this case, improves the mobility of the device and the flexibility of its use.

Devices in 5th generation (5G) cellular networks require very high precision phase and frequency synchronization. In practice, this means the accuracy of synchronizing end nodes with an accuracy better than 1 microsecond. It is then possible to access all services. There are several ways to achieve this. The first one is to build a dedicated synchronization network using PTPv2 or additionally White Rabbit technology. Unfortunately, despite the possibility of using part of the existing network infrastructure using PTP, the implementation of this solution is very expensive. An alternative solution is to synchronize all nodes to the GNSS.

In this paper, we show that it is possible to obtain synchronization times lower than for a CSAC generator while ensuring comparable or higher quality for rubidium generators, an example of which is the LPFRS generator considered in this paper [2].

II. METHOD

Global navigation satellite systems have been chosen as the synchronization signal source because GNSS signals are globally available and can be received from several independent systems, often based on different technologies.

Even temporary unavailability of a signal from one system, e.g., GPS, will not cause a loss of synchronization. The use of GNSS systems is possible at no additional charge.

In the research, rubidium and cesium oscillators were used as local oscillator. They belong to the group of highly stable oscillators. This paper assumed that the daily frequency instability of the oscillators under study is not greater than 10^{-9}. It is assumed that in the event of loss of the synchronization signal and the inability to tune the oscillator frequency, which leads to the transition of the device into a holding state, it is possible to meet current telecommunications standards for at least several hours.

The requirements for the fast synchronization of frequencies and phases of high-stability oscillators to signals from global navigation satellite systems are formulated as follows:

1. The output signal must meet the standards on MTIE and TDEV for the Primary Reference Time Clock (PRTC B).

2. The condition from the first point should be obtained as soon as possible.

3. In the synchronized state, maximum quality should be achieved, i.e., MTIE and TDEV values should be minimized.

4. The transition of the algorithm into the HOLDOVER state is to take place on the basis of data before the input signal disappears.

5. Return from HOLDOVER to the synchronized state after the input signal return as soon as possible.

Several intermediate steps were performed to find the optimal algorithm. The most important include:

- characterization of the reference signals from global navigation satellite systems for different receivers,
- identification experiments determining mathematical models in the space of state variables for atomic oscillators,
- implementation and comparison of phase noise reduction methods,
- finding the optimal parameters for the Kalman filter [3],
- implementation preprocessing techniques, including dynamic reset of the initial phase difference [4].

The block diagram of the proposed algorithm is shown in Figure 1. The first block is a phase detector that measures the phase difference between the 1PPS signal from a GNSS receiver and the signal from the local oscillator.

Then the measurement results are transferred to the OUTLIER block, which removes gross errors using the median filter. This block protects the rest of the algorithm from unwanted action caused by a significant measurement error. The MAV IN block is an input filter of the moving average type applied to reduce the level of input noise. The next block of the system is the Kalman filter. The optimal filter parameters have been determined in the work [3]. Thanks to the previously used MAV filter, the noise has been reduced to a level enabling the application of a two-dimensional model of the atomic clock. The Kalman filter provides denoised information about the phase of the system, as well as informs about the rate of phase changes. This data is used to choose a particular control algorithm, depending on the system's state.
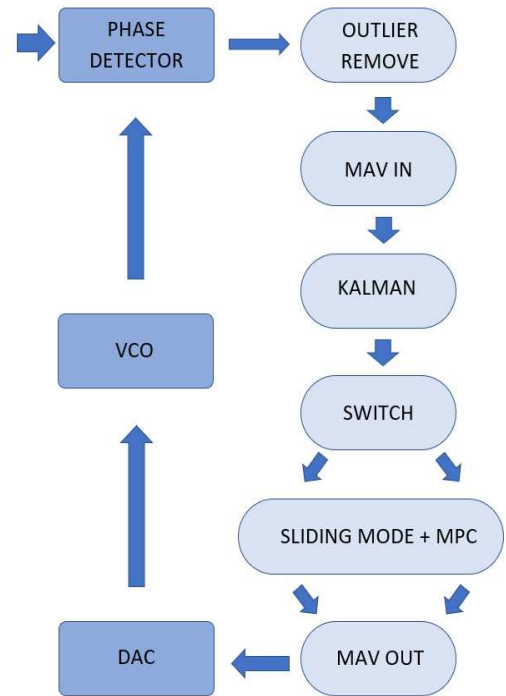

Fig. 1. Diagram of the algorithm for fast synchronization of high-stability oscillators to the GNSS signal

The state vector for the oscillator synchronization system has two state variables [3, 5]:

$$x(n) = \begin{bmatrix} x_{ph}(n) \\ x_{dph}(n) \end{bmatrix}, \qquad (1)$$

where $x_{ph}(n)$ maps the phase of the object, and $x_{dph}(n)$ is the derivative of $x_{ph}(n)$ describing the rate of change of this phase. This set of variables was chosen for the study because we aim to synchronize both phase and frequency.

The two algorithms were combined since it was impossible to meet all the requirements for a control algorithm by a homogeneous structure. A SWITCH block is a set of rules that select a given algorithm depending on the current phase and frequency error. Estimates of these values are derived from the Kalman filter.

After starting the system and completing the phase reset procedure, if the phase error exceeds the assumed 10 ns, the sliding control marked in the diagram as SLIDING MODE works. The sliding algorithm sets the minimum or maximum control value depending on whether the phase error is positive or negative. As a result, the phase error is reduced as quickly as possible. The control law is as follows [6]:

$$\text{if } ph(n) > 10 \ ns, \ then \ u(n) = \max u \qquad (2)$$

$$\text{if } ph(n) < -10 \ ns, \ then \ u(n) = \min u \qquad (3)$$

where $ph(n)$ maps the phase of the object, and $u(n)$ is the control voltage. The phase is read from the output of the Kalman filter.

When the phase error is less than the assumed 10 ns, the system switches to the Model Predictive Control (MPC)

algorithm, which ensures that PRTC B requirements on MTIE and TDEV are met. During the operation of this block, a correction is made to the stored code word previously applied for frequency synchronization during the last control process. Predictive control for the state variable model is LQR algorithm modification, where the control cost optimization is calculated for a finite number of steps M. The prediction and control horizons are the parameters determined at the initial stage of the predictive control procedure. The prediction horizon is the number of steps forward for which we determine the system's behavior for the adopted model in the space of state variables, while the control horizon is the number of steps ahead for which we are looking for optimal control. These values are not considered algorithm-tuning parameters. The algorithm can be properly tuned for correct values of horizons only.

The MPC uses an alternative extended cost function [7, 8]:

$$J(u) = \sum_{n=0}^{M}[x(n)^T \boldsymbol{Q_s} x(n) + u(n)^T \boldsymbol{R_s} u(n) +$$

$$\Delta u(n)^T \boldsymbol{R_\Delta} \Delta u(n)] \qquad (4)$$

where $\boldsymbol{Q_s}$ is a matrix of weights describing the cost of changing the state, $\boldsymbol{R_s}$ is a matrix describing the cost of changing control, $\Delta u(n)$ describes the control change in a given step, and the $\boldsymbol{R_\Delta}$ is the cost matrix of the rate of change of the control value. Reducing the dynamics of changes at the input results in reducing changes at the output of the oscillator.

The last block of the algorithm is the moving average filter marked as MAV OUT. It minimizes the negative effect caused by the change of the control algorithm, i.e., a significant step change of the control word, especially visible when the algorithm exits the sliding control.

III. RESULTS OF EXPERIMENTS

After theoretical analysis, experiments were used to examine whether the presented algorithm meets the requirements described in the Introduction. In addition, long-term properties were also analyzed by calculating the TDEV and MTIE of the generated signal. The reduction of the initial phase error to less than 10 ns was assumed as the time to achieve synchronism.

In sliding operation, the time to reduce the initial phase error of 100 ns to less than 10 ns for the LPRFS rubidium oscillator was 46 s. The time to reduce the initial phase error of 15 ns to less than 10 ns for the LPFRS rubidium oscillator was 19 s. Initial phase error reduction plots are shown in Figures 2 and 3. For both cases, time was lower for LPFRS than for the CSAC.

The long-term results (TDEV and MTIE for chosen observation intervals) of the LPRFS generator for the MPC algorithm for prediction horizon 1020 steps and control horizon 1000 steps are shown in Table 1. For $\boldsymbol{R_s} = 1$ and $\boldsymbol{Q_s} = \boldsymbol{I}$ different values of the MPC algorithm parameter $\boldsymbol{R_\Delta}$ (cost of control input turn rate) were considered.
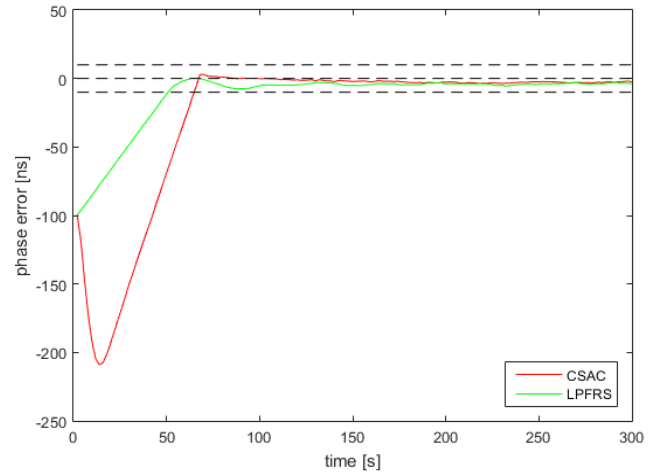

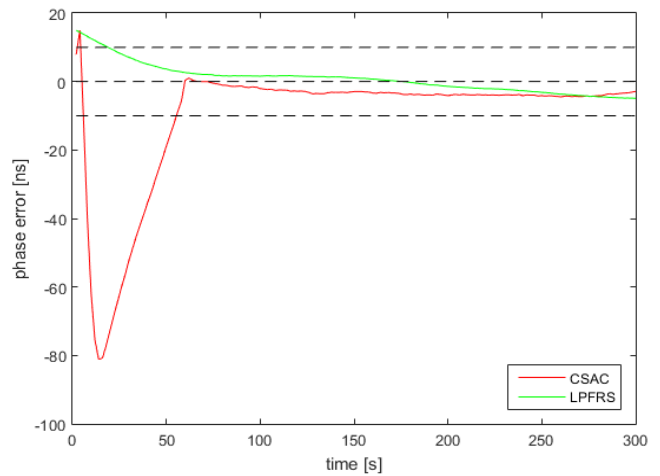Fig. 2. Example graph of –100 ns initial phase error reduction

Fig. 3. Example graph of 15 ns initial phase error reduction

The long-term results (TDEV and MTIE for chosen observation intervals) of the LPRFS generator for the MPC algorithm for a prediction horizon of length 1020 steps and control horizon of length 1000 steps are shown in Table I. The results are obtained independently of the initial phase error because they are calculated when the phase error is less than 10 ns and the system switches to the Model Predictive Control algorithm. Different values of the MPC algorithm parameter $\boldsymbol{R_\Delta}$ were considered.

The time constant is the only parameter that can be changed in the CSAC algorithm. According to the manufacturer's description [1], the system should be synchronized after a time equal to several time constants. In addition to the TDEV and MTIE results, the actual synchronization time is shown in the last column in Table II. The long-term behavior of the MPC algorithm for $R_\Delta = 240k$ is illustrated in Figures 4 and 5. Figure 4 contains the values of MTIE, and Figure 5 – the values of TDEV. In the same figures, the plots of MTIE and TDEV, respectively, for the CSAC oscillator for two synchronization times and the plot of ITU-T recommendation for the PRTC B clock were also contained.

R_Δ	TDEV [ns]			MTIE [ns]		
	10 s	*100 s*	*1000 s*	*10 s*	*100 s*	*1000 s*
30k	0.03	0.26	1.21	1.09	7.09	14.77
120k	**0.03**	**0.10**	**0.95**	**0.90**	**5.36**	**8.75**
240k	0.04	0.07	0.74	0.52	1.50	6.61
480k	0.07	0.07	1.61	0.75	3.69	18.40
720k	0.06	0.07	1.34	0.65	3.14	16.91
960k	0.06	0.07	0.77	0.89	4.29	11.58
1200k	0.06	0.07	1.51	0.64	2.77	14.59

TABLE II.   TDEV AND MTIE PARAMETERS FOR THE CONTROL ALGORITHM BUILT INTO THE CSAC OSCILLATOR

| Time Const [s]	TDEV [ns]			MTIE [ns]			Time syn. [s]
	10 s	*100 s*	*1000 s*	*10 s*	*100 s*	*1000 s*	
30	**0.40**	**0.75**	**0.92**	**8.23**	**16.46**	**16.46**	**60**
60	0.24	0.73	0.98	4.73	11.34	13.16	212
120	**0.15**	**0.54**	**0.97**	**2.02**	**5.39**	**9.28**	**302**
240	0.13	0.51	1.14	1.90	5.89	12.05	480
480	0.14	0.47	1.07	5.16	6.48	15.11	2216
960	0.14	0.45	1.55	4.55	5.63	17.04	7052
1920	0.12	0.43	1.49	4.42	6.53	12.57	9067
3640	0.32	0.47	1.74	4.92	7.13	18.19	10075
7680	0.44	0.46	1.48	4.33	7.61	12.26	38537
10000	0.21	0.47	1.5	3.82	5.81	21.29	20000
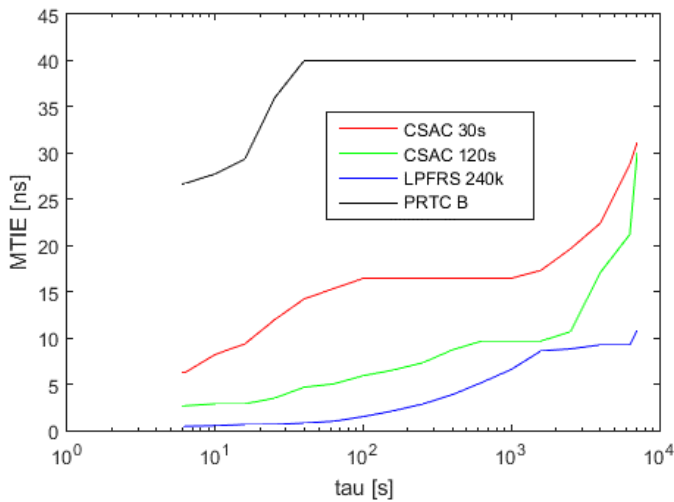
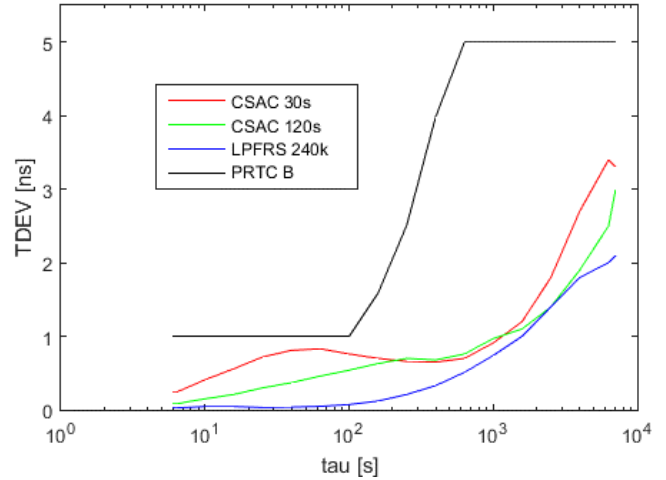Fig. 4. Sample plots of MTIE values compared to the PRTC B limit

Fig. 5. Sample plots of TDEV values compared to the PRTC B limit

IV. CONCLUSIONS

The paper proposes an algorithm for fast frequency and phase synchronization to the 1PPS signal from the GNSS system. The algorithm was tested for the LPRFS generator, representing a broad class of rubidium oscillators available on the market. The main result of the work is that with the proposed algorithm, it is possible to obtain synchronization times lower than for algorithms built into the CSAC oscillator while ensuring comparable quality. Alternatively, we can provide better output signal quality for the same synchronization time as the CSAC.

REFERENCES

[1] Microchip, "SA.45s Space Chip-Scale Atomic Clock (CSAC)," product information, 2020. Available: http://ww1.microchip.com/downloads/en/DeviceDoc/FTC-CSAC-r1-00002982C.pdf

[2] Spectratime, "Low Cost & Profile Frequency Rubidium Standard (LPFRS)," product information, Nov. 6, 2014. Available: https://xdevs.com/doc/SpectraTime/lpfrs_manual1.pdf

[3] P. Kubczak, J. Nikonowicz and Ł. Matuszewski, "Kalman Filter Design for Fast Synchronization of a High-Stability Rubidium Oscillator," *2019 Signal Processing: Algorithms, Architectures, Arrangements, and Applications (SPA)*, Poznan, Poland, 2019, pp. 77-80, doi: 10.23919/SPA.2019.8936821.

[4] P. Kubczak, M. Kasznia and M. Jessa, "Preprocessing for fast synchronization of high-stability oscillators disciplined by GNSS 1 PPS signal," *2018 European Frequency and Time Forum (EFTF)*, Turin, Italy, 2018, pp. 234-239, doi: 10.1109/EFTF.2018.8409040.

[5] J. -f. Wu, Y. -h. Hu, Z. -m. He, W. -f. Jing, H. -c. Lv and J. -l. Li, "The study of GPS Time Transfer based on extended Kalman filter, " *2013 Joint European Frequency and Time Forum & International Frequency Control Symposium (EFTF/IFC)*, Prague, Czech Republic, 2013, pp. 819-822, doi: 10.1109/EFTF-IFC.2013.6702097.

[6] J. K. Pieper, "First order dynamic sliding mode control," *Proceedings of the 37th IEEE Conference on Decision and Control (Cat. No.98CH36171)*, Tampa, FL, USA, 1998, pp. 2415-2420 vol.3, doi: 10.1109/CDC.1998.757768.

[7] O. Gonzales and A. Rosales, "Robust MPC Tuning by Quadratic Weights Online Estimation of the Cost Function through Extended Kalman Filter," *2018 International Conference on Information Systems and Computer Science (INCISCOS)*, Quito, Ecuador, 2018, pp. 49-54, doi: 10.1109/INCISCOS.2018.00015.

[8] A.K. Singh, B.C. Pal, "An extended linear quadratic regulator for LTI systems with exogenous inputs," Automatica, 2017, vol. 76, pp. 10-16.